Pergamon

Int. J. Solids Structures Vol. 35, No. 11, pp. 1075–1097, 1998

0020–7683/98 $19.00 + .00

PII: S0020–7683(97)00109–1

TRANSIENT CONCENTRATED THERMAL/MECHANICAL LOADING OF THE FACES OF A CRACK IN A COUPLED-THERMOELASTIC SOLID

H. G. GEORGIADIS
Mechanics Division, Department of Engineering Science, National Technical University of Athens, 1 Konitsis Street, Zographou 15773, Greece

L. M. BROCK
Department of Engineering Mechanics, University of Kentucky, 467 Anderson Hall, Lexington, KY 40506-0046, U.S.A.

and

A. P. RIGATOS
Mechanics Division, School of Engineering, Campus Box 422, Aristotle University of Thessaloniki, 54006 Thessaloniki, Greece

(*Received* 3 *September* 1996; *in revised form* 7 *March* 1997)

Abstract—A near-tip, transient, coupled thermoelastodynamic solution is presented for the plane stress/strain problem of a crack subjected to a concentrated thermal and/or mechanical loading, which is suddenly and symmetrically applied to the crack faces. Interest is focused on the stress field in the immediate vicinity of the crack during a small time-interval right after the application of loading and, therefore, the cracked body is considered of infinite extent and the crack itself of semi-infinite length. The loading consists of a pair of line heat sources or sinks (thermal loading) placed at the crack faces and/or a pair of equal, but opposite, line concentrated normal forces (mechanical loading) applied on the crack faces. These loadings may have an arbitrary time dependence (our analysis can deal with such cases), but here only the case of a step-function variation (the loadings act suddenly on the faces and are maintained there for all subsequent time) has been worked out. The thermoelastic wave propagation problem, which contains a characteristic length associated with the forcing function, is solved exactly in the time Laplace-transform domain by an analytic-function method. The inversion of the time Laplace-transformed stress intensity factor is carried out through a numerical technique. The present solution provides the Green's function for thermoelastic cracked bodies under more general spatially non-uniform loadings. © 1998 Elsevier Science Ltd.

1. INTRODUCTION

Within the framework of elastodynamic fracture mechanics, a considerable body of literature has been devoted to the study of stress-wave diffraction by stationary cracks. Such a problem is encountered when rapidly varying loads are applied to a nominally elastic body that contains stress concentrators, such as narrow cuts or slits and, therefore, the computation of the field requires that inertia effects be taken into account. When a wave disturbance reaches the crack edge, a non-uniform scattered field radiates out behind longitudinal and shear wavefronts. The governing equations are of hyperbolic type and the associated transient wave fields differ markedly from corresponding equilibrium (static) fields. A typical elastodynamic analysis usually aims at determining the crack tip stress intensity factor as a function of time and loading/geometry/material parameters. Of course, such information is essential for a better understanding of the response and fracture behavior of dynamically-loaded structural components [see e.g. basic discussions by Achenbach (1971); Achenbach and Brock (1975); Brock (1975); Chen and Sih (1977); Atkinson (1977, 1986); and Freund (1990); and some recent developments by Brock (1989, 1991); Jiang and Knowles (1989); Brock and Wu (1990); Lee and Freund (1990); Georgiadis, 1991; Georgiadis *et al.* (1991a, 1991b); Georgiadis and Brock (1993, 1994)].

In contrast to the intensive investigation into the above elastodynamic problem and the multitude of relative papers, only a few studies exist dealing with the more general thermoelastodynamic problem concerning thermally and/or mechanically activated disturbances in a cracked coupled-thermoelastic solid (Kassir *et al.*, 1986; Chen and Weng, 1991; Brock, 1992, 1995a, 1995b; Atkinson and Craster, 1992; Chen and Kuo, 1994). The latter situation is encountered when thermal and/or mechanical loads are rapidly applied on a cracked body, which is both thermally conducting and elastically deformable. In this way, transient thermoelastic disturbances give rise to high elevation of the stresses at the near-tip region of a pre-existing stationary crack which, just as in the non-thermal (purely elastic) case, may trigger crack extension and eventual failure. Notice that in this class of problems both inertial and thermal-coupling effects are taken into account according to the coupled thermoelastodynamic theory of Biot (1956) [see also Lessen (1956); Chadwick (1960); Carlson (1972)]. It is expected, of course, that such considerations will be essential to problems dealing with cracks in a non-stationary thermal/mechanical environment in which there is an interaction between thermal and mechanical fields. The associated results can be useful in the design of components which must withstand differential change in temperature.

The purpose of the present work is therefore to investigate a basic problem lying within the above-described framework of thermoelastodynamic fracture mechanics. This is the plane stress/strain problem of an unbounded thermoelastic solid containing a half-plane crack, the faces of which are subjected to the transient action of a pair of, symmetrically situated w.r.t. the crack plane, line concentrated thermal and/or mechanical loadings (see Fig. 1). The thermal sources (sinks) generate (absorb) heat at constant rate per unit time and unit length along a straight line parallel to the crack front, whereas the mechanical sources consist of equal, but opposite, normal forces which tend to separate the crack faces. This type of spatially non-uniform loading involves a characteristic length, which is the distance L between the point of application of the concentrated loading and the crack tip, thus introducing a certain mathematical difficulty in the course of obtaining an analytical solution. In particular, it gives rise to a non-standard functional equation in the double Laplace-transform (LT) domain that contains a term with exponentially unbounded behavior at infinity in the spatial-transform plane. It turns out then, that this behavior precludes application of the conventional Wiener–Hopf method (Noble, 1958; Roos, 1969) because the entire function resulting by the standard decoupling procedure (through the use of analytic continuation and Liouville's theorem) is an infinite-degree polynomial, whose unknown coefficients cannot be obtained by the disposed physical conditions. Nevertheless, this situation can be treated with the analytic-function technique of Georgiadis and Brock (1993), which is based on contour integration, Cauchy's integral and residue theorems, Jordan's lemma and Abel-Tauber theorems.

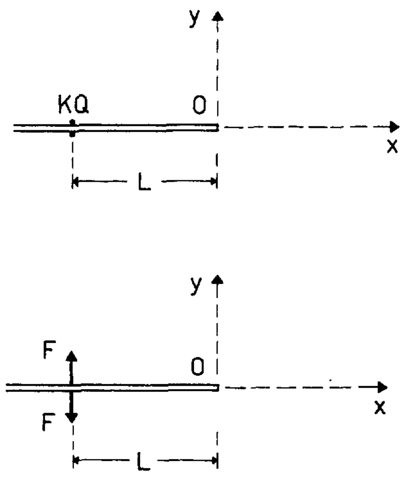

Fig. 1. Concentrated thermal (a) or mechanical (b) loading on the faces of a semi-infinite crack in an unbounded solid which is both thermally conducting and elastically deformable.

In this way, an exact solution is obtained in the time (one-sided) LT domain which allows the derivation of useful qualitative clues about the variation of the stress intensity factor at the crack tip. Also, results in the physical time domain are obtained by using the Stehfest (1970) numerical LT inversion technique. It is finally mentioned that we have taken the time dependence of loading to be a Heaviside step function. Of course, since the present solution is the Green's function of the problem, solutions corresponding to more general loadings in time and/or space can be obtained by numerical integration (of the convolution type) of the present fundamental solution.

Here, as is also the case in several crack–wave interaction problems examined earlier, attention is confined to the near-tip stress field for a small time-interval immediately after the action of loading and, therefore, we may assume that the boundaries of the body recede to infinity and the crack acts in effect as being of semi-infinite length. This is justified by the observation that even if thermal signals are transmitted with an infinite "speed", these disturbances at early times are indeed negligible at points not so close to the source [see for a relative discussion concerning transient thermal contacts the works by Barber (1989), Barber *et al.* (1989), and Georgiadis *et al.* (1991)].

In concluding this Introduction, some closely related works involving rapidly loaded fully-coupled thermoelastic bodies with cracks should be noted. Kassir *et al.* (1986) studied the problem of a finite-length crack under both thermal and mechanical uniform loading in an unbounded solid through dual integral equations and the Miller–Guy numerical LT inversion technique. Brock (1992, 1995a, 1995b) treated, in an exact manner, configurations of semi-infinite cracks under mechanical uniform impact loadings in unbounded solids studying dislocation generation and the formation of zones of slip/diffusion mechanisms near the crack edges. Atkinson and Craster (1992) introduced an invariant integral to analyze time dependent, but spatially uniform loadings of a thermoelastic strip containing a semi-infinite crack. Chen and Weng (1991), and Chen and Kuo (1994) utilized finite elements to analyze an edge-cracked strip problem, which was also the subject of several other investigations employing non-inertial and uncoupled thermoelasticity [see e.g. Nied (1983, 1987)]. Finally, no attempt is made here to systematically quote other papers on thermoelastic crack problems which are based on simpler non-inertial and/or uncoupled thermomechanical theories. Typical of such work and further references can be found in Nied (1983, 1987), Barber and Comninou (1983), and Kokini and Long (1988).

2. GOVERNING EQUATIONS AND INTEGRAL TRANSFORMS

The material behavior considered in the present analysis is linear coupled thermoelastodynamic (Biot, 1956; Lessen, 1956; Chadwick, 1960; Carlson, 1972). In the absence of body forces and heat sources inside the medium, the governing equations are written as

$$\sigma_{ij} = \lambda\delta_{ij}u_{l,l} + \mu(u_{i,j} + u_{j,i}) - (3\lambda + 2\mu)\delta_{ij}\psi_0\theta \tag{1}$$

$$\mu u_{i,jj} + (\lambda + \mu)u_{j,ji} - (3\lambda + 2\mu)\psi_0\theta_{,i} = \rho\frac{\partial^2 u_i}{\partial t^2} \tag{2}$$

$$K\theta_{,ii} - \rho c_{\mathrm{U}}\frac{\partial\theta}{\partial t} - (3\lambda + 2\mu)\psi_0 T_0\frac{\partial(u_{i,i})}{\partial t} = 0 \tag{3}$$

where indicial notation is employed with $(\,)_{,i}$ denoting x_i-differentiation, δ_{ij} is the Kronecker delta, $\sigma_{ij}(=\sigma_{ji})$ is the stress tensor, u_i is the displacement vector, λ and μ are Lamé's constants, ψ_0 is the coefficient of linear expansion, $\theta(=T-T_0)$ is the change in temperature, T is the current temperature, T_0 is the initial temperature, ρ is the mass density, t is the time, K is the thermal conductivity, and c_{U} is the specific heat at constant deformation.

Equation (1) is the thermoelastic Hooke's law, whereas eqns (2) and (3) can be regarded as, respectively, Navier–Cauchy equations and heat conduction equation with source terms. It may also be noticed that the third term in the left-hand side of both eqns (2) and (3) arises from the interaction of elastic deformation with heat conduction. Shear waves, however, are not affected by the ability of the medium to conduct heat; only dilatational waves are modified by thermal straining and, conversely, only mechanical energy expended in volume changes is converted into heat (see e.g. Chadwick, 1960).

In the present analysis, two-dimensional bodies under in-plane loadings are considered and, therefore, a plane stress/strain formulation is relevant. Especially in the plane-stress case, we further assume that the lateral surfaces of the plate are insulated. Then, the governing eqns (1)–(3) can be written under the following form by utilizing an (x, y) Cartesian coordinate system

$$\frac{1}{\mu}\sigma_x = m^2\frac{\partial u_x}{\partial x} + (m^2-2)\frac{\partial u_y}{\partial y} + \psi\theta \tag{4a}$$

$$\frac{1}{\mu}\sigma_y = (m^2-2)\frac{\partial u_x}{\partial x} + m^2\frac{\partial u_y}{\partial y} + \psi\theta \tag{4b}$$

$$\frac{1}{\mu}\sigma_{xy} = \frac{\partial u_x}{\partial y} + \frac{\partial u_y}{\partial x} \tag{4c}$$

$$\nabla^2 u_x + \frac{\partial[(m^2-1)\Delta + \psi\theta]}{\partial x} - m^2\frac{\partial^2 u_x}{\partial s^2} = 0 \tag{5a}$$

$$\nabla^2 u_y + \frac{\partial[(m^2-1)\Delta + \psi\theta]}{\partial y} - m^2\frac{\partial^2 u_y}{\partial s^2} = 0 \tag{5b}$$

$$\frac{K}{\mu}\nabla^2\theta - \frac{c_U m}{V_2}\frac{\partial\theta}{\partial s} + \psi T_0 V_1\frac{\partial\Delta}{\partial s} = 0 \tag{6}$$

where $m \equiv V_1/V_2 > 1$ with $V_1 \equiv [(\lambda+2\mu)/\rho]^{1/2}$ being the dilatational-wave speed in the absence of thermal effects and $V_2 \equiv (\mu/\rho)^{1/2}$ being the shear-wave speed, $\psi \equiv \psi_0(4-3m^2) < 0$, $\nabla^2 \equiv (\partial^2/\partial x^2) + (\partial^2/\partial y^2)$ is the Laplace operator, $\Delta \equiv (\partial u_x/\partial x) + (\partial u_y/\partial y)$ is the dilatation, and $s \equiv V_1 t$ is the normalized time. All field quantities above are functions of x, y and s. This alternative (Brock, 1995b) to the standard (Chadwick, 1960) formulation offers some advantage to operations presented in the sequel.

For convenience in the subsequent analysis, the s and x dependence in the governing equations and the boundary/initial conditions are suppressed through the use of, respectively, one- and two-sided Laplace transforms. In this subsection thus, general expressions for the double transformed displacements, stresses and temperature in the thermoelastic half-plane $(-\infty < x < \infty, y \geqslant 0)$ are given. These expressions will facilitate in the sequel the formulation of pertinent mixed boundary value problems. We note, in passing, that integral-transform analyses for half-plane domains within the coupled thermoelastodynamic theory were previously done by Boley and Tolins (1962) and Massalas *et al.* (1985) among others, with particular reference, however, to uniform boundary conditions at the half-plane surface (i.e. essentially, within 1-D formulations).

The transforms and their corresponding inversion operations are

$$F(x,y,p) = \int_0^\infty f(x,y,s)\cdot \mathrm{e}^{-ps}\,\mathrm{d}s \tag{7a}$$

$$f(x,y,s) = \frac{1}{2\pi i}\int_{\mathrm{Br}} F(x,y,p)\cdot \mathrm{e}^{ps}\,\mathrm{d}p, \tag{7b}$$

and

$$F^*(q,y,p) = \int_{-\infty}^{\infty} F(x,y,p)\cdot \mathrm{e}^{-pqx}\,\mathrm{d}x \tag{8a}$$

$$F(x,y,p) = \frac{p}{2\pi i}\int_{\mathrm{Br}} F^*(q,y,p)\cdot \mathrm{e}^{pqx}\,\mathrm{d}q \tag{8b}$$

with the convention followed whereby a function which is to be transformed is denoted by a small letter, its one-sided LT by the corresponding capital letter, and its two-sided LT by an asterisk. In eqns (7b) and (8b), Br denotes the Bromwich path in pertinent complex planes. When working in the double transform plane, however, p can be treated as a real and positive parameter, but q is generally a complex variable (see e.g. Carrier *et al.*, 1966).

Successive application of eqns (7a) and (8a) to the field eqns (5) and (6), and considering zero initial conditions for the displacements, particle velocities and temperature change results in a coupled set of ordinary differential equations having the following general solutions that are bounded for $y > 0$ (Brock, 1995b)

$$pU_x^* = -q\bar{A}_+ - q\bar{A}_- + \bar{A}_\beta \tag{9}$$

$$pU_y^* = \alpha_+\bar{A}_+ + \alpha_-\bar{A}_- + \frac{q}{\beta}\bar{A}_\beta, \tag{10}$$

$$\frac{\psi}{m^2}\Theta^* = M_+\bar{A}_+ + M_-\bar{A}_- \tag{11}$$

where

$$\bar{A}_+ = A_+(p,q)\cdot \mathrm{e}^{-p\alpha_+ y}, \quad \bar{A}_- = A_-(p,q)\cdot \mathrm{e}^{-p\alpha_- y}, \quad \bar{A}_\beta = A_\beta(p,q)\cdot \mathrm{e}^{-p\beta y} \tag{12a,b,c}$$

with A_+, A_- and A_β being arbitrary functions, and

$$\alpha_+ \equiv \alpha_+(p,q) = (m_+^2 - q^2)^{1/2}, \quad \alpha_- \equiv \alpha_-(p,q) = (m_-^2 - q^2)^{1/2}, \quad \beta \equiv \beta(q) = (m^2 - q^2)^{1/2} \tag{13a,b,c}$$

$$2m_\pm = \left[(1+\tau^{-1/2})^2 + \frac{\varepsilon}{\tau}\right]^{1/2} \pm \left[(1-\tau^{-1/2})^2 + \frac{\varepsilon}{\tau}\right]^{1/2} \tag{14}$$

$$M_\pm = m_\pm^2 - 1, \quad M_+M_- = -\frac{\varepsilon}{\tau}, \quad \tau = hp. \tag{15a,b,c}$$

Also, two important quantities have been introduced in eqns (14) and (15), namely the dimensionless coupling constant ε and the thermoelastic characteristic length h which are defined by Chadwick (1960)

$$\varepsilon = \frac{T_0}{c_\mathrm{U}}\left(\frac{\psi V_2}{m}\right)^2, \quad h = \frac{KV_2}{\mu m c_\mathrm{U}}. \tag{16a,b}$$

These quantities, for usual conducting materials (like aluminum, copper, lead, titanium and 4340 steel), have orders of magnitude $\varepsilon = \mathcal{O}(10^{-2})$ and $h = \mathcal{O}(10^{-10}\ m)$.

The general transformed solution is completed by recording the double transformed stresses, which are obtained by using eqns (4) and (7)–(11)

$$\frac{1}{\mu}\Sigma_x^* = T_+\bar{A}_+ + T_-\bar{A}_- + 2q\bar{A}_\beta \tag{17}$$

$$\frac{1}{\mu}\Sigma_y^* = -T\bar{A}_+ - T\bar{A}_- - 2q\bar{A}_\beta \tag{18}$$

$$\frac{1}{\mu}\Sigma_{xy}^* = 2q\alpha_+\bar{A}_+ + 2q\alpha_-\bar{A}_- - \frac{T}{\beta}\bar{A}_\beta \tag{19}$$

where

$$T_+ = 2\alpha_+^2 - m^2, \quad T_- = 2\alpha_-^2 - m^2, \quad T = 2\beta^2 - m^2 \equiv m^2 - 2q^2. \tag{20a,b,c}$$

Finally, the necessary restriction [in view of the chosen solution forms (9)–(12)] that $\mathrm{Re}(\alpha_+)$, $\mathrm{Re}(\alpha_-)$, $\mathrm{Re}(\beta) \geqslant 0$ in the cut q-plane leads to the fact that the functions defined in eqn (13) should exhibit branch cuts along $(\bar{m} < |\mathrm{Re}(q)| < \infty, \mathrm{Im}(q) = 0)$, where $\bar{m} = m_+$, m_- and m, respectively. Also, we record here the two possible arrangements of m_+, m_- and m w.r.t. their magnitude. Of course, this information along with the latter one will enable us to define the regions of analyticity of various functions appearing in subsequent analyses. The quantities m_+ and m_- are p-dependent, whereas m is constant. In view of their definitions, it turns out that

$$m_- < m_+ < m \quad \text{for } \tau_m < \tau \equiv hp \tag{21a}$$

$$m_- < m < m_+ \quad \text{for } hp \equiv \tau < \tau_m \tag{21b}$$

where $\tau_m = [m^2(1+\varepsilon) - 1][m^2(m^2-1)]^{-1}$. It should be noted, however, that case (21a) is rather impractical for the present study, since it corresponds to an extremely small time interval. For instance, by considering the material constants of titanium ($\mu = 43.00842$ GPa, Poisson's ratio $\nu = 0.32$, $\rho = 4650$ Kg m^{-3}, $V_1 = 5900$ m s^{-1}, $V_2 = 3041.2371$ m s^{-1}, $m = 1.94$, $\psi_0 = 9.7 \times 10^{-6}$ m m^{-1} °C^{-1}, $c_U = 490$ J Kg^{-1} °C^{-1}, $K = 10.9$ W m^{-1} °C^{-1}) which will be utilized to extract numerical results here and assuming an initial temperature $T_0 = 20$°C, case (21a) occurs only when $t < 5.18 \times 10^{-13}$ s. We note, in passing, that the above values give the estimations $\varepsilon = 0.000506$ for the coupling constant and $h = 8.1 \times 10^{-10}$ m for the thermoelastic characteristic length. In most conducting materials also, inequality (21a) holds for times less than 10^{-10} s. Thus, in what follows we shall confine attention to the case (21b) by considering time scales, after loading the cracked body, within the interval 10^{-12} s $< t < 10^{-5}$ s for $L = 0.05$ m.

3. THERMAL LOADING OF THE CRACKED BODY

3.1. *Problem statement*

Consider a thermally conducting linearly elastic body occupying the region $(-\infty < x < \infty, -\infty < y < \infty)$ and containing a stationary semi-infinite crack situated along the plane $(-\infty < x < 0, y = 0)$, see Fig. 1(a). The material is stress-free, at rest and at constant temperature T_0 everywhere for $t < 0$. At $t \equiv s/V_1 = 0$, the crack faces are suddenly subjected to a concentrated heat flux at $(x = -L, y = \pm 0)$. From that source (sink), heat is generated (absorbed) at constant rate KQ per unit time and unit length along a straight line parallel to the crack front. Q is a multiplier expressed in degrees of temperature and it is positive (negative) in the case of a source (sink).

Because of symmetry with respect to the plane $y = 0$, the problem can be viewed as a half-plane problem with the body occupying the region $(-\infty < x < \infty, 0 < y < \infty)$. Then, the associated initial/boundary value problem must satisfy the following conditions.

3.1.1. *Boundary and initial conditions.*

$$\frac{\partial\theta(x,0,s)}{\partial y} = -Q\cdot\delta(x+L)\cdot H(s/V_1) \quad \text{for } -\infty < x < \infty \tag{22a}$$

$$\sigma_{xy}(x,0,s) = 0 \quad \text{for } -\infty < x < \infty \tag{22b}$$

$$\sigma_y(x,0,s) = 0 \quad \text{for } -\infty < x < 0 \tag{22c}$$

$$u_y(x,0,s) = 0 \quad \text{for } 0 < x < \infty \tag{22d}$$

$$u_x(x,y,0) = \partial u_x(x,y,0)/\partial s = u_y(x,y,0) = \partial u_y(x,y,0)/\partial s = \theta(x,y,0) = 0 \tag{22e}$$

where $\delta(\cdot)$ and $H(\cdot)$ stand for the Dirac delta distribution and the Heaviside step function, respectively.

3.1.2. *Edge conditions.*

$$\sigma_y(x,0,s) = \mathcal{O}(x^{-\gamma}) \quad \text{with } \gamma < 1 \quad \text{for } x \to 0^+ \tag{23a}$$

$$u_y(x,0,s) = \mathcal{O}(1) \quad \text{for } x \to 0^- \tag{23b}$$

which guarantees that the near-tip stress and displacement fields will not be so singular as to correspond to sources of radiated energy. Integrable kinetic and potential energy is, in turn, a necessary condition for solution uniqueness (Knops and Payne, 1970; Achenbach, 1973).

3.1.3. *Finiteness conditions at remote regions.*

$$|\Sigma_y(x,0,p)| < \mathscr{A}\cdot\exp(-q_\Sigma x) \quad \text{for } x \to +\infty \tag{24a}$$

$$|U_y(x,0,p)| < \mathscr{B}\cdot\exp(q_U x) \quad \text{for } x \to -\infty \tag{24b}$$

where $\Sigma_y(x,0,p)$ and $U_y(x,0,p)$ are the one-sided Laplace transforms of the unknown cleavage stress and crack–surface displacement at the crack line, and $\mathscr{A}$, $\mathscr{B}$, q_Σ and q_U are positive quantities. The above relations are a direct consequence of the asymptotic behavior of the time Laplace-transformed Green's functions of the wave and heat-conduction equations, and they guarantee that the diffraction field at infinity consists of outgoing signals only. The latter asymptotic behavior of Green's functions is $\mathcal{O}(\exp(-pqr))$ for the wave equation and $\mathcal{O}(\exp(-p^{1/2}qr))$ for the heat–conduction equation, as $r \equiv (x^2+y^2)^{1/2} \to \infty$. Thus, even in the case of heat–conduction, where temperature signals are transmitted at an infinite speed, there is a decay of source-induced solutions at infinity like $\mathcal{O}(\exp(-r^2/4t))$.

The objective here is the determination of the stress field near to the crack tip for the problem defined by eqns (4)–(6) and (22)–(24). In particular, exact analysis will provide $\Sigma_y(x \to 0^+,0,p)$, whereas $\sigma_y(x \to 0^+,0,V_1 t)$ will be obtained by numerically inverting the Laplace-transformed cleavage stress.

3.2. *Analysis*

It may be observed from the problem statement that the functions $\sigma_y(x,0,s)$ and $u_y(x,0,s)$ are unknown in the intervals $0 < x < \infty$ and $-\infty < x < 0$, respectively. Accordingly, we define the following half-line transforms of their one-sided LTs

$$\Sigma^*_{y+}(q,p) \equiv \int_0^\infty \Sigma_y(x,0,p)\cdot e^{-pqx}\,dx \quad \text{for } -\frac{q_\Sigma}{p} < \mathrm{Re}(q) \tag{25a}$$

$$\Sigma_y(x,0,p) = \frac{p}{2\pi i}\int_{\mathrm{Br}_1} \Sigma^*_{y+}(q,p)\cdot e^{pqx}\,dq \quad \text{for } 0 < x < \infty \tag{25b}$$

$$U^*_{y-}(q,p) \equiv \int_{-\infty}^0 U_y(x,0,p)\cdot e^{-pqx}\,dx \quad \text{for } \mathrm{Re}(q) < \frac{q_U}{p} \tag{26a}$$

$$U_y(x,0,p) = \frac{p}{2\pi i}\int_{\mathrm{Br}_2} U^*_{y-}(q,p)\cdot \mathrm{e}^{pqx}\,\mathrm{d}q \quad \text{for } -\infty < x < 0 \tag{26b}$$

where, of course, conditions (24) were employed in order to define the half-planes of analyticity of the functions $\Sigma^*_{y+}(q,p)$ and $U^*_{y-}(q,p)$ in the complex q-plane. These as yet unknown functions are to be determined through the analytic-function method of Georgiadis and Brock (1993). In light of definitions (7), (8), (25) and (26), the transformed boundary conditions (22a–d) give

$$\frac{\partial\Theta^*(q,0,p)}{\partial y} = -\frac{Q\cdot \mathrm{e}^{Lpq}}{p} \tag{27a}$$

$$\Sigma^*_{xy}(q,0,p) = 0 \tag{27b}$$

$$\Sigma^*_y(q,0,p) = \Sigma^*_{y+}(q,p) \tag{27c}$$

$$U^*_y(q,0,p) = U^*_{y-}(q,p). \tag{27d}$$

Combining now the general expressions (10), (11), (18) and (19) for the transformed functions appearing in the left-hand sides of (27) with eqns (27) provides four equations containing five unknown functions. Further, by eliminating A_+, A_- and A_β from this system, a single equation results containing Σ^*_{y+} and U^*_{y-}

$$\Sigma^*_{y+}(q,p)+\left(\frac{1}{\alpha_+}-\frac{1}{\alpha_-}\right)\cdot\Lambda(q,p)\cdot \mathrm{e}^{Lpq} = \frac{\mu p}{m^2(M_+-M_-)}\cdot\frac{D(q,p)}{\alpha_+\alpha_-}\cdot U^*_{y-}(q,p) \tag{28}$$

where

$$\Lambda(q,p) = \frac{\mu KQ\cdot T(q)}{m^2(M_+-M_-)p^2} \tag{29}$$

and $D(q,p)$ is the kernel function given by

$$D = \alpha_- M_- R_+ - \alpha_+ M_+ R_- \tag{30}$$

with

$$R_+ = 4q^2\alpha_+\beta + T^2,\quad R_- = 4q^2\alpha_-\beta+T^2. \tag{31a,b}$$

We notice that the functions $R_+(q,p)$ and $R_-(q,p)$ can be viewed as the thermoelastic counterparts of the classical (purely elastic or non-thermal) transformed Rayleigh function defined [see e.g. Achenbach (1973)] by $R \equiv 4q^2(1-q^2)^{1/2}\beta + T^2$. In fact, R_+ reduces to R when thermal effects are neglected (i.e. $\varepsilon = h = 0$) and the coupled thermoelastodynamic governing equations (1) and (2) degenerate into the standard elastodynamic equations. Unlike R, however, R_+ and R_- involve branch cuts which shift with p, a fact indicating that the thermoelastic Rayleigh-wave velocity is time dependent. This will soon become clearer.

It should also be noted that, in view of the regions of definition of the various functions appearing in eqn (28), this equation holds only along a vanishingly thin vertical strip in the q-plane which, in fact, degenerates into the $\mathrm{Im}(q)$-axis.

The main task now is to produce separate equations for both the yet unknown functions Σ^*_{y+} and U^*_{y-}, which enter the single eqn (28), through a decoupling procedure. This is possible by supplying eqn (28) with results obtained by using analytic-function theory. In particular, the method introduced by Georgiadis and Brock (1993) will be followed. At this point, we emphasize that the conventional Wiener–Hopf technique (Carrier *et al.*, 1966; Roos, 1969) is not directly applicable to eqn (28) because of the inconvenient (unbounded as $|q| \to \infty$) behavior of the forcing term e^{Lpq}, as discussed in the Introduction. Thus, the usual argument of analytic continuation in conjunction with Liouville's theorem (which are the basic ingredients of the Wiener–Hopf technique) is of no use in this case. Instead, the different approach followed here utilizes simple contour integration, an exact kernel-factorization, Cauchy's integral and residue theorem, and Jordan's lemma.

To proceed further we need to perform a factorization of the kernel $D(q,p)$ in the q-plane. If the following function is introduced

$$S \equiv \frac{D}{M(M_+ - M_-)(q^2 - q_R^2)\alpha_+} \tag{32}$$

which possesses the desired asymptotic property $S(q,p) \to 1$ as $|q| \to \infty$, and the standard technique of factorization through the use of Cauchy's integral theorem is then applied to it, the result will be

$$S = S_+ \cdot S_- \tag{33}$$

where

$$S_\pm(q,p) = \exp\left(\frac{1}{\pi}\cdot\int_{m_-}^{m} \tan^{-1}\left[\frac{a_-}{\alpha_+}\left(\frac{M_-}{M_+} - \alpha_+\frac{4z^2\beta}{T^2\lambda_+}\right)\right]\cdot\frac{dz}{z\pm q}\right.$$
$$\left. + \frac{1}{\pi}\cdot\int_{m}^{m_+} \tan^{-1}\left[\frac{a_-}{\alpha_+}\left(\frac{M_+}{M_-} + a_-\frac{4z^2b}{T^2\lambda_-}\right)^{-1}\right]\cdot\frac{dz}{z\pm q}\right) \tag{34}$$

with the newly introduced symbols defined as

$$M = 2(m^2 - 1) \tag{35}$$

$$a_+ \equiv a_+(z,p) = (z^2 - m_+^2)^{1/2}, \quad a_- \equiv a_-(z,p) = (z^2 - m_-^2)^{1/2}, \quad b \equiv b(z) = (z^2 - m^2)^{1/2} \tag{36a,b,c}$$

$$q_R(p) = \frac{m^2[\lambda_- + (m_-/m_+)\lambda_+]^{1/2}}{S_\pm(q=0,p)\cdot M^{1/2}} \tag{37}$$

$$\lambda_+ = M_-/(M_- - M_+), \quad \lambda_- = M_+/(M_+ - M_-). \tag{38a,b}$$

In the above equations, S is an analytic function in the q-plane cut along $(m_- < |\mathrm{Re}(q)| < m_+, \mathrm{Im}(q) = 0)$, and S_+ and S_- are analytic functions in the overlapping half-planes $\mathrm{Re}(q) > -m_-$ and $\mathrm{Re}(q) < m_-$, respectively. Also, $q = \pm q_R$ (with $m < q_R < m_+$) are the zeros of the function (D/α_+) defined in eqn (30) and they correspond, in the physical plane, to thermoelastic Rayleigh waves propagating along the crack surfaces. The associated velocity (V_1/q_R) depends on p (i.e. on time), as eqn (37) implies, clearly indicating a dispersive character of the surface wave due to energy loss in the thermomechanical process. However, the latter velocity varies in practice only slightly with time. For instance, by using again the material constants of titanium and assuming an initial temperature $T_0 = 20°\mathrm{C}$ it is found that $q_R = 2.22996$ and $m_+ = 2.33265$ for $t = 5.18 \times 10^{-13}$ s, whereas $q_R = 2.23001$ and $m_+ = 16204.3$ for $t = 2.5 \times 10^{-5}$ s. This can be explained in view of the fact that, in general, while there is a strong shear contribution (which remains unaffected by thermal effects) to the Rayleigh disturbances, the dilatational part of them is very weak [see e.g. Viktorov (1967)]. Finally, in the non-thermal limit ($\varepsilon = h = 0$) it can be shown that $q_R \to (V_1/V_R)$, where V_R is the classical Rayleigh-wave velocity [see e.g. Achenbach (1973)].

With the factorization (33) in hand, eqn (28) can be written now as

$$\left[\Sigma_{y+}^* + \left(\frac{1}{\alpha_+} - \frac{1}{\alpha_-}\right)\cdot \Lambda \cdot e^{Lpq}\right]\cdot \frac{(m_- + q)^{1/2}}{(a+q_R)\cdot S_+} = \frac{\mu M p}{m^2}\cdot \frac{(q-q_R)\cdot S_-}{(m_- - q)^{1/2}}\cdot U_{y-}^* \tag{39}$$

which holds only along the Im(q)-axis. Our decoupling procedure will concentrate, in particular, on Σ_{y+}^*, since here the ultimate objective is the determination of the stress intensity factor at the crack tip. The first step in applying this procedure is changing the variable from q to ω, then dividing both sides of (39) by $2\pi i(\omega - q)$, and finally integrating the resulting functions over the imaginary axis iIm(ω) by also taking the point q to lie on the right half-plane Re(ω) > 0 only. The foregoing operations give

$$\begin{aligned}
&\frac{1}{2\pi i}\int_{-i\infty}^{i\infty} \frac{\Sigma_{y+}^*(\omega,p)\cdot(m_- + \omega)^{1/2}}{(\omega+q_R)\cdot S_+(\omega,p)\cdot(\omega-q)}\mathrm{d}\omega \\
&\quad + \frac{1}{2\pi i}\int_{-i\infty}^{i\infty} \frac{e^{Lp\omega}\cdot(m_- + \omega)^{1/2}\cdot\Lambda(\omega,p)}{(m_+^2 - \omega^2)^{1/2}(\omega+q_R)\cdot S_+(\omega,p)\cdot(\omega-q)}\mathrm{d}\omega \\
&\quad - \frac{1}{2\pi i}\int_{-i\infty}^{i\infty} \frac{e^{Lp\omega}\cdot(m_- + \omega)^{1/2}\cdot\Lambda(\omega,p)}{(m_-^2 - \omega^2)^{1/2}(\omega+q_R)\cdot S_+(\omega,p)\cdot(\omega-q)}\mathrm{d}\omega \\
&= \frac{\mu M p}{m^2}\cdot\frac{1}{2\pi i}\int_{-i\infty}^{i\infty} \frac{U_{y-}^*(\omega,p)\cdot(\omega-q_R)\cdot S_-(\omega,p)}{(m_- - \omega)^{1/2}(\omega-q)}\mathrm{d}\omega.
\end{aligned} \tag{40}$$

The afore-mentioned restriction in the placement of the q points in the complex plane is, however, particularly convenient for obtaining the desired $\lim_{x\to 0^+}\Sigma_y(x,0,p)$-expression, since the latter is associated with $\lim_{|q|\to\infty}\Sigma_{y+}^*(q,p)$, where q is taken along paths in the right half-plane Re(q) > 0.

Next, working on the integral in the right-hand side of eqn (40), we observe that for $|\omega| \to \infty$ the integrand meets the conditions for applying Jordan's lemma (Carrier *et al.*, 1966), since $S_-(\omega,p) \to 1$ and eqn (23b) should be satisfied (the latter being used along with the Abel-Tauber theorem (Roos, 1969)). We also observe that the integrand is an analytic function in the left half-plane Re(ω) < 0. Therefore, by applying contour integration with deforming the integration path so as to include a large semi-circle at infinity in the left half-plane and by also applying Jordan's lemma to this integral, we conclude by Cauchy's theorem that it actually vanishes when q is a point of the right half-plane Re(ω) > 0.

Then by employing again contour integration and Jordan's lemma on the first integral of the left-hand side of eqn (40), and by closing the integration path with a large semi-circle at infinity in the right half-plane, we obtain the following result through Cauchy's integral formula

$$\begin{aligned}
\frac{\Sigma_{y+}^*(q,p)\cdot(m_- + q)^{1/2}}{(q+q_R)\cdot S_+(q,p)} &= \frac{1}{2\pi i}\int_{-i\infty}^{i\infty} \frac{e^{Lp\omega}\cdot\Lambda(\omega,p)}{(m_- - \omega)^{1/2}(\omega+q_R)\cdot S_+(\omega,p)\cdot(\omega-q)}\mathrm{d}\omega \\
&\quad - \frac{1}{2\pi i}\int_{-i\infty}^{i\infty} \frac{e^{Lp\omega}\cdot(m_- + \omega)^{1/2}\cdot\Lambda(\omega,p)}{(m_+^2 - \omega^2)^{1/2}(\omega+q_R)\cdot S_+(\omega,p)\cdot(\omega-q)}\mathrm{d}\omega \quad (q \text{ in } \mathrm{Re}(\omega) > 0).
\end{aligned} \tag{41}$$

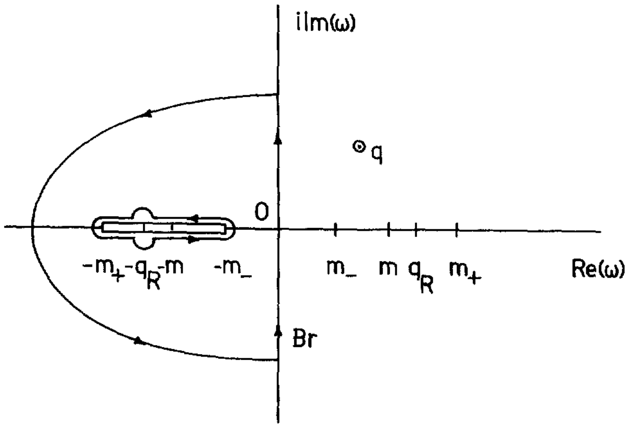

Fig. 2. Deformation of contour and branch cuts for the first integral in eqn (41).

Finally, the two integrals in eqn (41) can formally be evaluated by closing the integration path with a large semi-circle at infinity in the left half-plane. One can observe that the integrands in both integrals meet the requirements for applying Jordan's lemma and that the branch cut $(-m_+ < \mathrm{Re}(\omega) < -m_-, \mathrm{Im}(\omega) = 0)$ should be introduced for the first integral. Then, application of Cauchy's integral and residue theorem leads to the expression (see also Figs 2 and 3)

$$\Sigma^*_{y+}(q,p) = \frac{(q+q_R)\cdot S_+(q,p)}{(m_-+q)^{1/2}}\cdot\left[\frac{1}{\pi}\,⨍_{m_-}^{m_+}\frac{e^{-Lp\omega}\cdot\Lambda(\omega,p)\cdot S_+(\omega,p)}{(m_-+\omega)^{1/2}(\omega-q_R)\cdot|S(\omega,p)|\cdot(q+\omega)}\,d\omega + \frac{e^{-Lpq_R}\cdot(q_R-m_-)^{1/2}\cdot\Lambda(q_R,p)\cdot S_+(q_R,p)}{(m_+^2-q_R^2)^{1/2}\cdot|S(q_R,p)|\cdot(q+q_R)}\right] \quad (42)$$

where $⨍$ denotes Cauchy principal-value integration (the Rayleigh-wave pole occurs in the integrand), and

$$|S(q,p)| \equiv [M(M_+-M_-)(q^2-q_R^2)]^{-1}\cdot[M_-(4q^2|\alpha_+||\beta|+T^2)|\alpha_-|(|\alpha_+|)^{-1}-M_+(4q^2|\alpha_-||\beta|+T^2)]. \quad (43)$$

Equation (42) is the final result of the analysis in the double LT domain. This expression may provide, through two LT inversions, the crack-line stress $\sigma_y(x,0,s)$. Since, however,

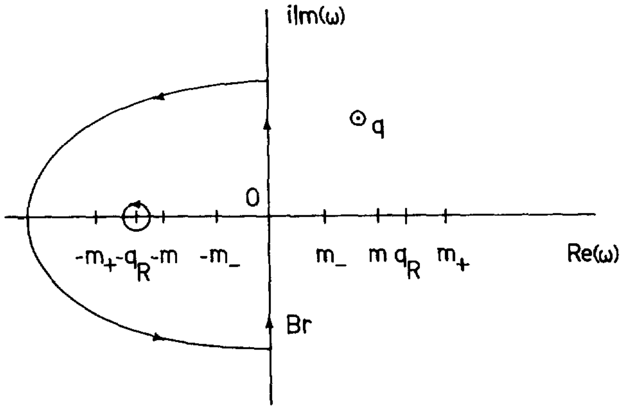

Fig. 3. Deformation of contour and branch cuts for the second integral in eqn (41).

exact analytical inversions of eqn (42) appear to be formidable, we shall resort to asymptotics and numerics for returning to the original space/time domain. In particular, an asymptotic analytical inversion according to eqn (25b) will give $\Sigma_y(x \to 0^+, y = 0, p)$, and then, a numerical inversion of the one-sided LT via the Stehfest (1970) technique will provide values of $\sigma_y(x \to 0^+, y = 0, t)$ and its intensity at the crack edge. A final comment regarding the suitability of the standard Wiener–Hopf technique is now in order. First, one may observe that a sum splitting (i.e. additive decomposition) of the term $\{[(1/\alpha_+) - (1/\alpha_-)] \cdot \Lambda \cdot (m_- + q)^{1/2}/[(q + q_R) \cdot S_+]\} \cdot e^{Lpq}$ in eqn (39) according to the way described in, e.g., Section 9.4.1 of Achenbach's (1973) treatise is not feasible because the necessary condition that $\{\cdots\} \cdot e^{Lpq} = \mathcal{O}(|q|^{-\gamma})$ for $|q| \to \infty$, with $\gamma > 0$, is not met here. As is clearly exposed in Achenbach (1973), p. 369, his condition (9.49) is absolutely needed in order to apply Jordan's lemma and get his eqns (9.48), (9.50) and (9.51). However, such an additive decomposition would be possible, by means of Theorem B, p. 13 in Noble's (1958) treatise, if eqn (39) were to hold inside a vertical strip in the q-plane and not only along the line $\mathrm{Re}(q) = 0$. Second, if the Plemelj formula is employed for a sum splitting, as is standard in the case of an equality along a line, the term $(1/2) \cdot \{\cdots\} \cdot e^{Lpq}$ will arise in the side which is analytic in $\mathrm{Re}(q) > 0$ prohibiting again the application of Liouville's theorem in obtaining the necessary order relations as $|q| \to \infty$.

3.3. *Basic asymptotic results*

The Abel-Tauber theorem [see e.g. Roos (1969), Achenbach (1973)] is utilized to obtain the singular part of stress, $\lim_{x \to 0^+} \Sigma_y(x, 0, p)$, from the large-$q$ expression of eqn (42), $\lim_{|q| \to \infty} \Sigma^*_{y+}(q, p)$. Indeed, by approximating $(q + \omega)$ by q and $(m_- + q)^{1/2}$ by $q^{1/2}$ in eqn (42), and by taking into account that $S_+(q, p) \to 1$, as $|q| \to \infty$, one finds

$$\lim_{|q| \to \infty} \Sigma^*_{y+}(q, p) = \frac{1}{(pq)^{1/2}} \cdot \frac{\mu K Q}{m^2 (M_+ - M_-) p^{3/2}} \cdot \left[\frac{1}{\pi} \int_{m_-}^{m_+} \frac{e^{-Lp\omega} \cdot (m^2 - 2\omega^2) \cdot S_+(\omega, p)}{(m_- + \omega)^{1/2} \cdot (\omega - q_R) \cdot |S(\omega, p)|} d\omega \right.$$
$$\left. + \frac{e^{-Lpq_R} \cdot (q_R - m_-)^{1/2} \cdot (m^2 - 2q_R^2) \cdot S_+(q_R, p)}{(m_+^2 - q_R^2)^{1/2} \cdot |S(q_R, p)|} \right] \quad (44)$$

from which an inversion according to eqn (25b) is readily obtained as

$$\lim_{x \to 0^+} \Sigma_y(x, 0, p) = \frac{1}{(\pi x)^{1/2}} \cdot \frac{\mu K Q}{m^2 (M_+ - M_-) p^{3/2}} \cdot [\cdots] \quad (45)$$

where the expression in brackets is the same as that in eqn (44).

Finally, the time (one-sided) Laplace transformed stress-intensity-factor (SIF) at the crack tip follows from its standard definition and eqn (45) as

$$K_I(p) \equiv \lim_{x \to 0^+} [(2\pi x)^{1/2} \cdot \Sigma_y(x, 0, p)] = \frac{2^{1/2} \mu K Q}{m^2 (M_+ - M_-) p^{3/2}}$$
$$\cdot \left[\frac{1}{\pi} \int_{m_-}^{m_+} \frac{e^{-Lp\omega} \cdot (m^2 - 2\omega^2) \cdot S_+(\omega, p)}{(m_- + \omega)^{1/2} \cdot (\omega - q_R) \cdot |S(\omega, p)|} d\omega + \frac{e^{-Lpq_R} \cdot (q_R - m_-)^{1/2} \cdot (m^2 - 2q_R^2) \cdot S_+(q_R, p)}{(m_+^2 - q_R^2)^{1/2} \cdot |S(q_R, p)|} \right] \quad (46)$$

which, in view of the discussion immediately following eqn (21), holds for $p < (\tau_m/h)$.

3.4. *Numerical results*

First, the behavior of the transformed SIF in eqn (46) is examined, and then, a numerical inversion is performed. Also, some asymptotic estimates allow drawing useful quantitative results. In all numerical work that follows, the material constants of titanium quoted earlier are employed and $L = 0.05\ m$ is taken.

For convenience, we consider a normalized transformed SIF defined as

$$K_{\mathrm{I}}^{\mathrm{norm}}(p) \equiv K_{\mathrm{I}}(p)\cdot\frac{\pi^{1/2}m^2}{2^{1/2}\mu KQ} = \frac{\pi^{1/2}}{(M_+ - M_-)p^{3/2}}\cdot[\cdots] \equiv F_1 + F_2 \tag{47}$$

where the expression in brackets is the same as that in eqns (44) and (46), and (F_1, F_2) denote, respectively, the integral and the exponential term (in these brackets) multiplied by their common factor $(\pi^{1/2}/(M_+ - M_-)p^{3/2})$. Figures 4 and 5 depict the variation of the functions F_1 and F_2 (i.e. the components of the normalized transformed SIF) with $(Lp)^{-1}$, where p is taken as a real and positive variable. Of course, this enables us to conclude about the qualitative behavior of their respective inverse functions vs time. Figures 6 and 7, also, depict the variation of the functions $F_3 \equiv |S(q_{\mathrm{R}}, p)|\cdot[S_+(q_{\mathrm{R}}, p)]^{-1}$ and $F_4 \equiv [M(M_+ - M_-)]^{-1}$ with $(Lp)^{-1}$, and one could observe that F_3 is rather independent on $(Lp)^{-1}$ (i.e. independent on time) taking the value 2.052 over a fairly wide range, whereas F_4 becomes vanishingly small very soon.

The normalized SIF, $k_{\mathrm{I}}^{\mathrm{norm}} \equiv k_{\mathrm{I}}(s = V_1 t)\cdot(\pi^{1/2}m^2/2^{1/2}\mu K\cdot|Q|)$ vs normalized time $(V_1 t/L)$, is shown in Figs 8 and 9, where, respectively, $Q < 0$ (heat flux is absorbed by an energy sink) and $Q > 0$ (heat flux is generated by an energy source). These graphs were generated by numerically inverting the transformed SIF via the Stehfest (1970) algorithm. The latter technique, which is particularly suitable when the variable of the one-sided LT is taken to be real, was recommended by the well-known survey study on LT inversion techniques of Davies and Martin (1979) and has extensively been utilized in transient crack

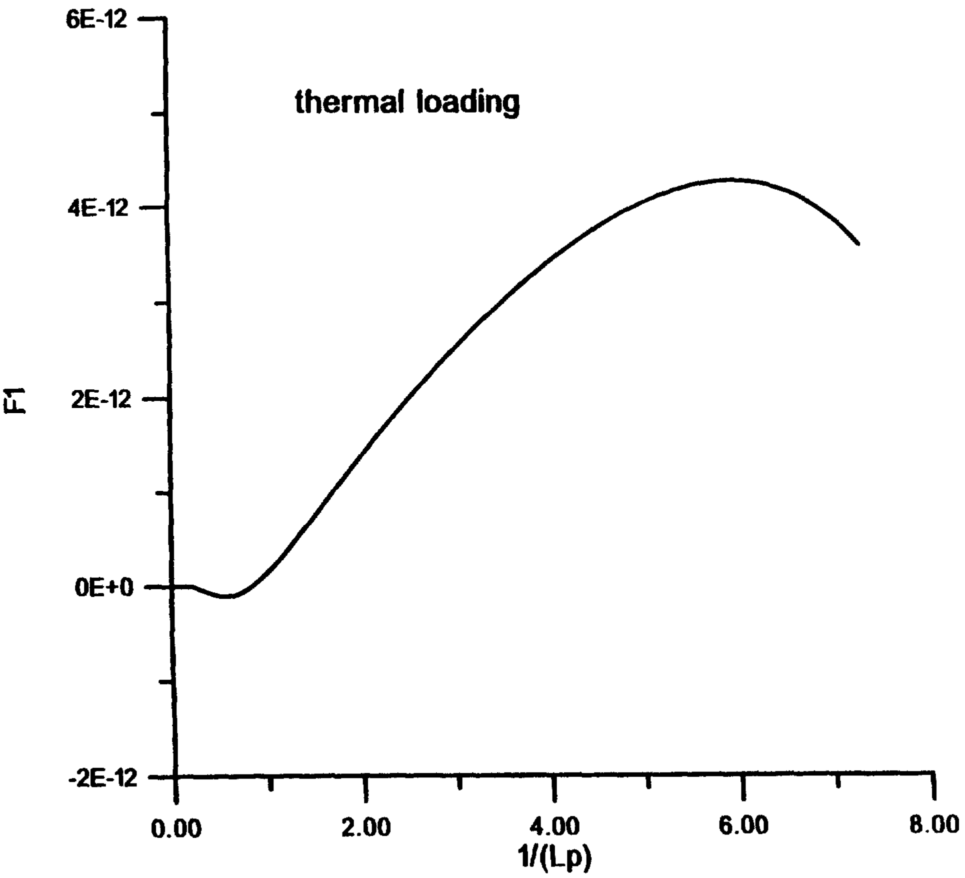

Fig. 4. Variation of the function F_1, as defined in eqn (47), with $(Lp)^{-1}$.

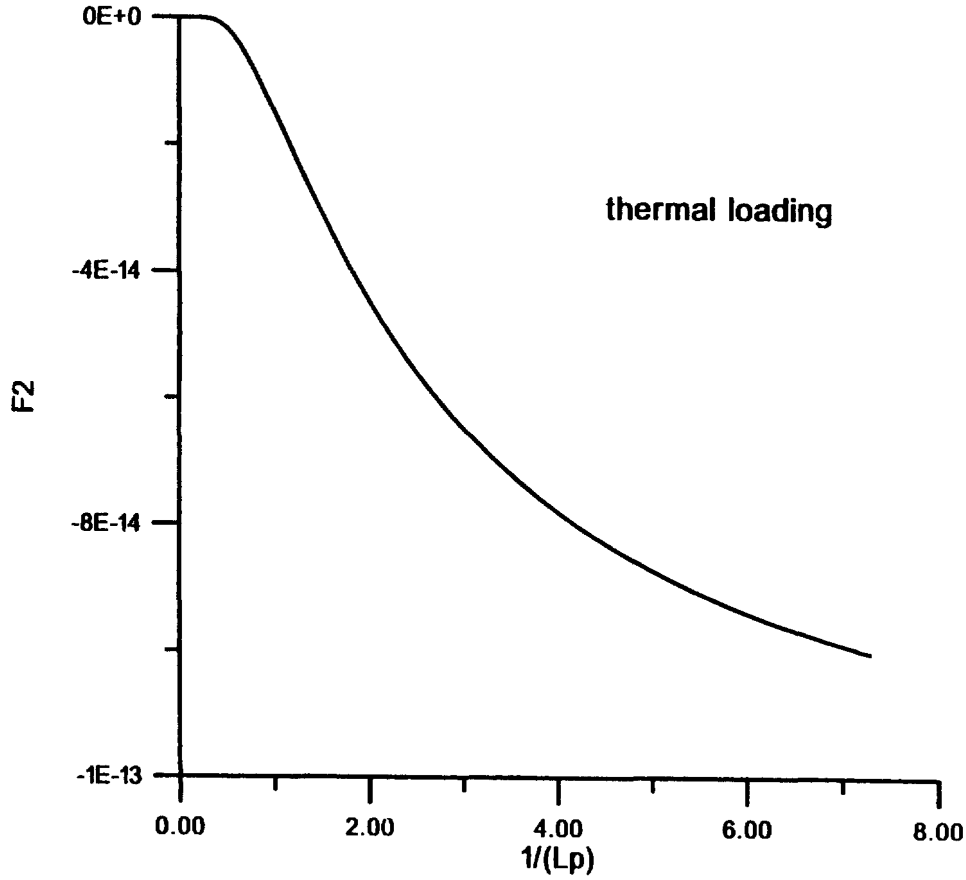

Fig. 5. Variation of the function F_2, as defined in eqn (47), with $(Lp)^{-1}$.

and stress-concentration problems [see e.g. Ang (1988), and Rajapakse and Gross (1995)]. Referring to eqn (7), the approximate inversion is given as

$$f(s) \cong \left(\frac{\ln 2}{s}\right) \cdot \sum_{n=1}^{N} c_n \cdot F\left(n \frac{\ln 2}{s}\right) \tag{48}$$

where

$$c_n = (-1)^{n+N/2} \cdot \sum_{k=[(n+1)/2]}^{\min(n,N/2)} \frac{k^{N/2}(2k)!}{(N/2-k)!k!(k-1)!(n-k)!(2k-n)!} \tag{49}$$

N is even (with $N = 18$ good convergence was generally obtained in our computations), and [] means the integer part of a number.

In both cases corresponding to Figs 8 and 9, our computations show that the SIF becomes unbounded at times near the time of arrival of the thermoelastic Rayleigh wave at the crack tip. This surface wave was generated at $(x = -L, y = 0, t = 0)$ due to the concentrated loading at the crack faces, and the arrival time is $t \cong Lq_R/V_1 \cong 2.23L/V_1$. After the arrival of the Rayleigh wave at the crack tip, the SIF tends gradually to its steady-state limit (which is zero) because the temperature field in the body tends again to a uniform state as time passes after the sudden application of the thermal loading.

The above behavior can also be predicted analytically by making use of the following approximations for the quantities m_+ and m_- and by considering the long-time (i.e. small p) limit. The approximations $m_+ \cong [(1+\varepsilon)/hp]^{1/2}$ and $m_- \cong (1+\varepsilon)^{-1/2}$ for $(s/h) \gg 1$ have a quite broad range of validity since the necessary conditions that $(s/h) \gg 1$ holds true (e.g. the restriction $(s/h) > 1000$) in most practical cases for times $t > \mathcal{O}(10^{-10}\,\mathrm{s})$ (Brock, 1995b).

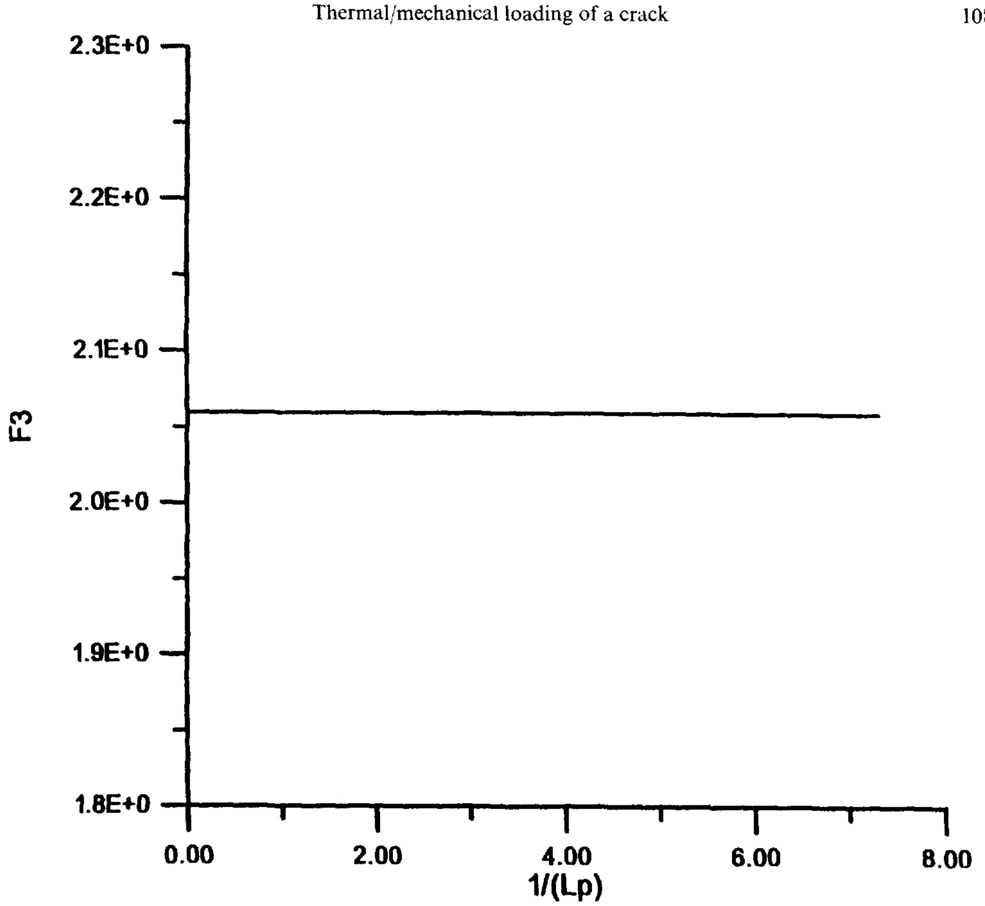

Fig. 6. Variation of the function $F_3 \equiv |S(q_R, p)| \cdot [S_+(q_R, p)]^{-1}$ with $(Lp)^{-1}$.

Then, it is found that the transformed SIF varies like $[(1+\varepsilon)^2 - hp]^{-1} \cdot [(1+\varepsilon) - q_R^2 hp]^{-1/2} \cdot e^{-Lq_R p}$ and at the limit

$$\lim_{p \to 0} K_1(p) \sim e^{-Lq_R p} \tag{50}$$

which upon inversion yields

$$\lim_{s \to \infty} k_1(s = V_1 t) \sim \delta(Lq_R - s) \tag{51}$$

predicting thus a spike of the SIF at the time of the thermoelastic Rayleigh-wave arrival at the crack tip, but a zero value afterwards.

A final comment pertains to the negative values of SIF occurring in some time intervals in the cases illustrated in Figs 8 and 9. These negative values indicate crack closure. However, we notice [see also Georgiadis and Brock (1994) and relative references therein] that the mathematical crack considered here is merely an idealization of the narrow slit of finite thickness (on the order of 0.003 m) normally found in experimental situations involving pre-cracked specimens. Therefore, it is reasonable to assume that no contact actually takes place although the crack surfaces tend to close during certain time intervals.

4. MECHANICAL LOADING OF THE CRACKED BODY

4.1. *Problem statement*

Consider again the thermally conducting linearly elastic body of Fig. 1(b). This body occupies the region $(-\infty < x < \infty, -\infty < y < \infty)$ and contains a stationary semi-infinite crack extending along $(-\infty < x < 0, y = 0)$. The material is stress-free, at rest and at

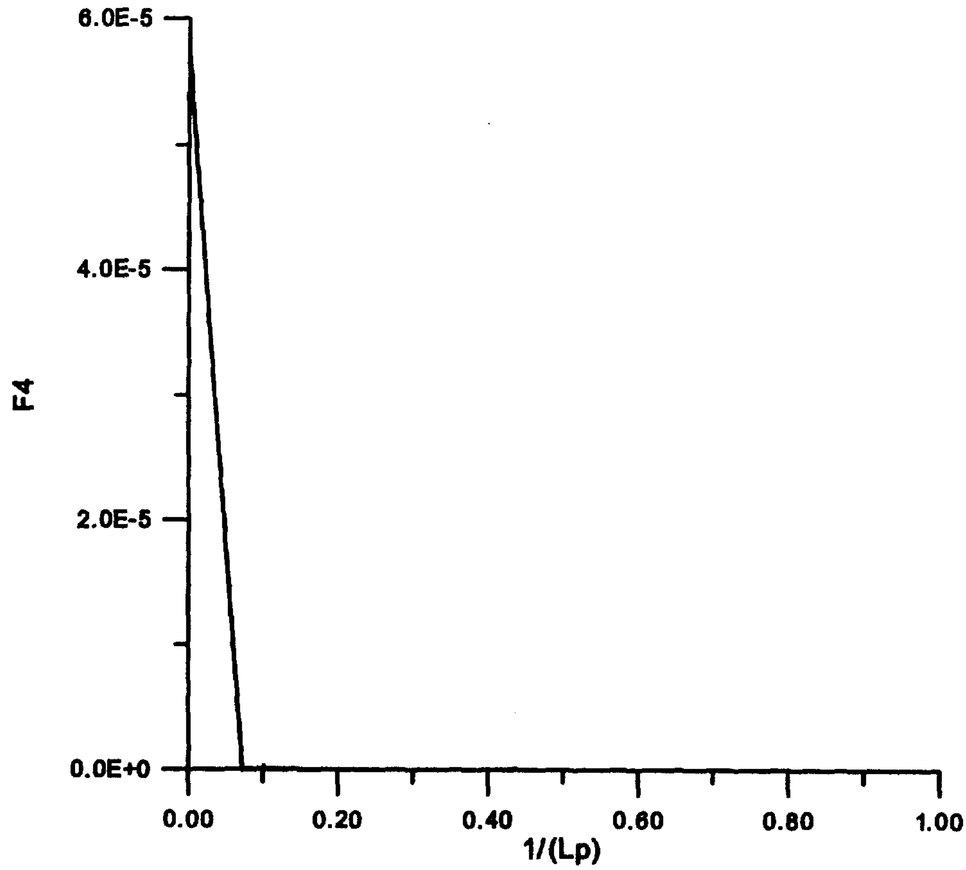

Fig. 7. Variation of the function $F_4 \equiv [M(M_+ - M_-)]^{-1}$ with $(Lp)^{-1}$.

constant temperature T_0 everywhere for $t < 0$. At $t \equiv s/V_1 = 0$, the crack faces are suddenly subjected to equal, but opposite, concentrated line normal forces F, which tend to separate the crack faces in an opening mode.

Because of symmetry with respect to the plane $y = 0$, the problem can be viewed as a half-plane problem with the body occupying the region $(-\infty < x < \infty, 0 < y < \infty)$. Then, the associated initial/boundary value problem must satisfy the edge and finiteness conditions stated in eqns (23) and (24), respectively (as for the thermal loading case), and the following boundary and initial conditions

$$\sigma_y(x,0,s) = -F \cdot \delta(x+L) \cdot H(s/V_1) \quad \text{for } -\infty < x < 0 \tag{52a}$$

$$\sigma_{xy}(x,0,s) = 0 \quad \text{for } -\infty < x < \infty \tag{52b}$$

$$u_y(x,0,s) = 0 \quad \text{for } 0 < x < \infty \tag{52c}$$

$$\frac{\partial \theta(x,0,s)}{\partial y} = 0 \quad \text{for } -\infty < x < \infty \tag{52d}$$

$$u_x(x,y,0) = \partial u_x(x,y,0)/\partial s = u_y(x,y,0) = \partial u_y(x,y,0)/\partial s = \theta(x,y,0) = 0 \tag{52e}$$

where F is expressed in dimensions of force per unit length.

As in the previous case, our objective now is the determination of the near-tip stress field for the problem defined by eqns (4)–(6), (23), (24) and (52). It is noted that in the absence of thermal effects (purely elastic response), the above problem is the classical diffraction crack problem of Freund (1974). Here, however, we follow a direct analytical scheme to solve the thermoelastic problem instead of Freund's superposition technique.

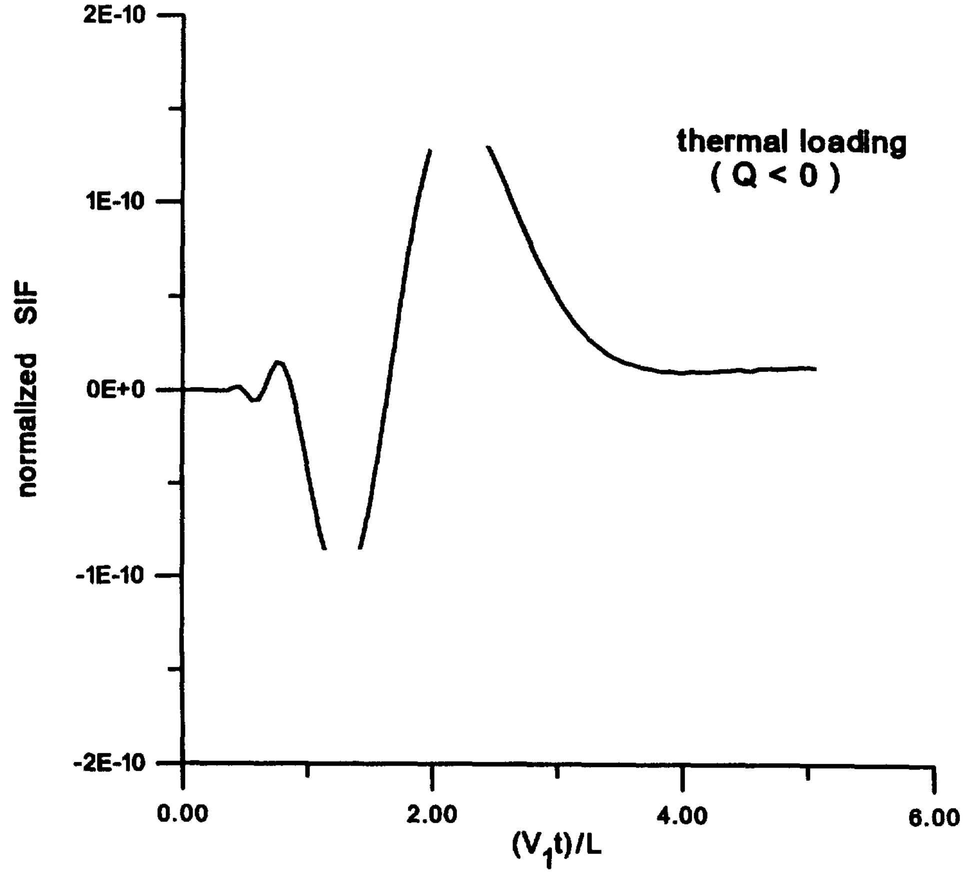

Fig. 8. History of the normalized SIF for thermal loading with $Q < 0$.

4.2. *Brief analysis and asymptotic results*

By following the same approach as in Section 3.2 of this paper, we can produce a functional equation containing the unknowns Σ^*_{y+} and U^*_{y-}

$$\Sigma^*_{y+}(q,p) - \frac{F\cdot e^{Lpq}}{p} = \frac{\mu p}{m^2(M_+ - M_-)}\cdot\frac{D(q,p)}{\alpha_+\alpha_-}\cdot U^*_{y-}(q,p) \tag{53}$$

where the kernel function $D(q,p)$ was given in eqn (30). Our analytic-function technique yields now the decoupled solution

$$\frac{\Sigma^*_{y+}(q,p)\cdot(m_- + q)^{1/2}}{(q+q_R)\cdot S_+(q,p)} = \frac{F}{2\pi ip}\int_{-i\infty}^{i\infty}\frac{e^{Lp\omega}\cdot(m_- + \omega)^{1/2}}{(\omega+q_R)\cdot S_+(\omega,p)\cdot(\omega-q)}\mathrm{d}\omega \quad (q\,\text{in}\ \mathrm{Re}(\omega) > 0). \tag{54}$$

The above integral can formally be evaluated by closing the integration path with a large semi-circle at infinity in the left half-plane. After introducing the branch cut $(-\infty < \mathrm{Re}(q) < -m_+, \mathrm{Im}(q) = 0)$, which is pertinent to the integrand, and using Jordan's lemma and Cauchy's residue theorem, we end up with the expression (see also Fig. 10)

$$\Sigma^*_{y+}(q,p) = \frac{F\cdot(q+q_R)\cdot S_+(q,p)}{p(m_- + q)^{1/2}}$$

$$\cdot\left[-\frac{1}{\pi}\int_{m_+}^{\infty}\frac{e^{-Lp\omega}\cdot(\omega-m_-)^{1/2}}{(\omega-q_R)\cdot S_-(\omega,p)\cdot(\omega+q)}\mathrm{d}\omega + \frac{e^{-Lpq_R}\cdot(q_R-m_-)^{1/2}\cdot S_+(q_R,p)}{|S(q_R,p)|\cdot(q_R+q)}\right]. \tag{55}$$

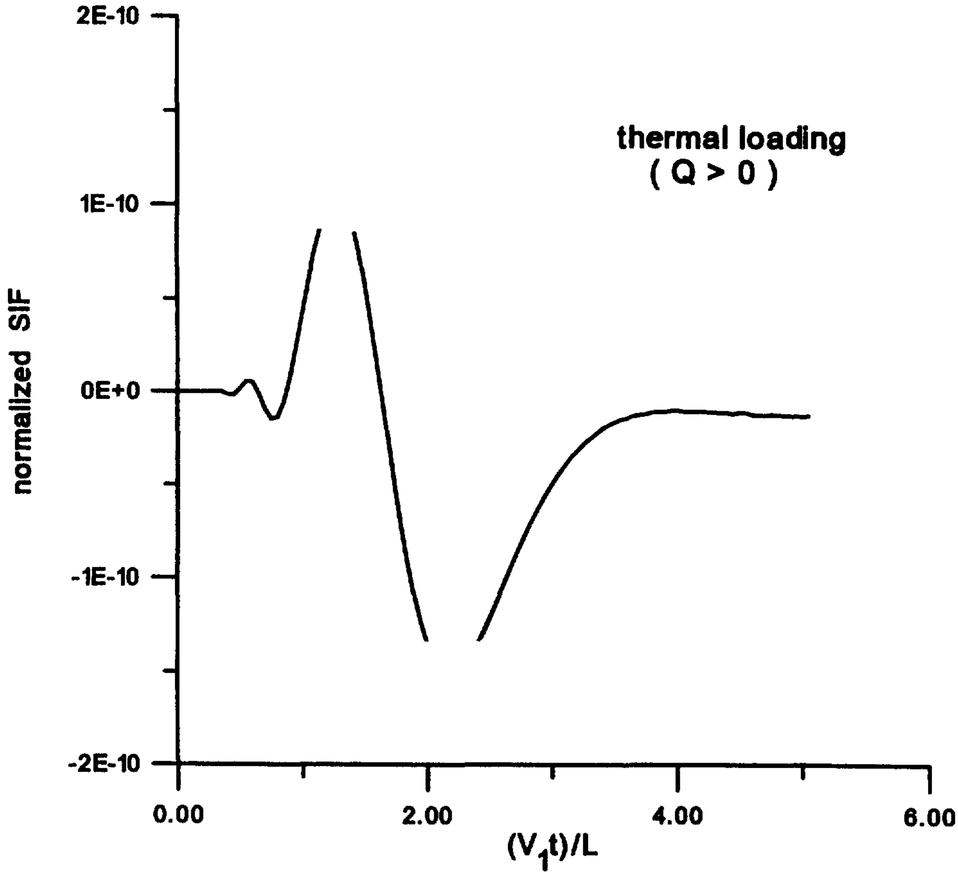

Fig. 9. History of the normalized SIF for thermal loading with $Q > 0$.

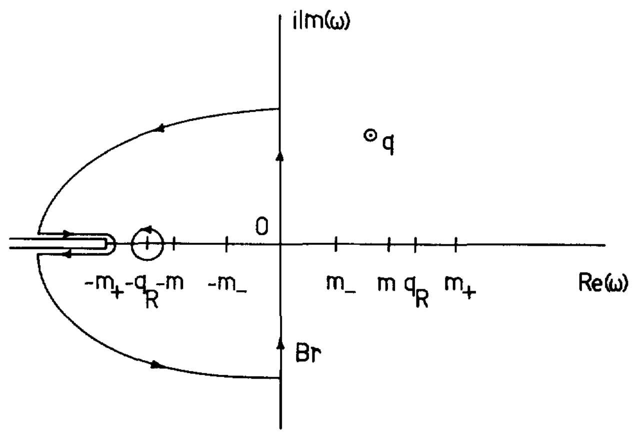

Fig. 10. Deformation of contour and branch cuts for the integral in eqn (54).

Again, this is an exact result for the double transformed cleavage stress. First, an exact, but asymptotic, inversion according to eqn (25b) gives $\Sigma_y(x \to 0^+, y = 0, p)$, and next, a numerical inversion according to eqn (7b) will follow. The former inversion is made possible by obtaining the large-q form of eqn (55) and by invoking the Abel-Tauber theorem. In particular, $(q+q_R)$ and $(q+\omega)$ are approximated by q, and the upper limit of the integral in eqn (55) is replaced by $(\infty-\zeta)$, where $(\infty-\zeta)$ is sufficiently large to ensure that

$$\frac{e^{-Lp\omega}\cdot(\omega-m_-)^{1/2}}{(\omega-q_R)\cdot S_-(\omega,p)} \to 0 \quad \text{as } \omega \to (\infty-\zeta). \tag{56}$$

The following expression is, therefore, obtained

$$\lim_{|q|\to\infty} \Sigma^*_{y+}(q,p) = \frac{1}{(pq)^{1/2}} \cdot \frac{F}{p^{1/2}} \cdot \left[-\frac{1}{\pi} \int_{m_+}^{\infty-\zeta} \frac{e^{-Lp\omega} \cdot (\omega - m_-)^{1/2}}{(\omega - q_R) \cdot S_-(\omega,p)} d\omega \right.$$
$$\left. + \frac{e^{-Lpq_R} \cdot (q_R - m_-)^{1/2} \cdot S_+(q_R,p)}{|S(q_R,p)|} \right] \quad (57)$$

and an immediate inversion follows giving

$$\lim_{|q|\to\infty} \Sigma^*_{y+}(q,p) = \frac{1}{(\pi x)^{1/2}} \cdot \frac{F}{p^{1/2}} \cdot [\cdots] \quad (58)$$

where the expression in brackets is the same as that in eqn (57). The former step can indeed be realized if we write the integral I in eqn (55) under the form

$$I = \int_{m_+}^{\infty-\zeta} \frac{e^{-Lp\omega} \cdot (\omega - m_-)^{1/2}}{(\omega - q_R) \cdot S_-(\omega,p) \cdot (\omega + q)} d\omega + \int_{\infty-\zeta}^{\infty} \frac{e^{-Lp\omega} \cdot (\omega - m_-)^{1/2}}{(\omega - q_R) \cdot S_-(\omega,p) \cdot (\omega + q)} d\omega \quad (59)$$

and consider the limit as $|q| \to \infty$. Also, one should observe that the integrand in eqn (57) rapidly tends to zero for $\omega \gg q_R$.

Finally, the time (one-sided) Laplace transform SIF at the crack tip results from its standard definition and eqn (58)

$$K_I(p) \equiv \lim_{x\to 0^+} [(2\pi x)^{1/2} \cdot \Sigma_y(x,0,p)] = \frac{2^{1/2}F}{p^{1/2}} \cdot \left[-\frac{1}{\pi} \int_{m_+}^{\infty-\zeta} \frac{e^{-Lp\omega} \cdot (\omega - m_-)^{1/2}}{(\omega - q_R) \cdot S_-(\omega,p)} d\omega \right.$$
$$\left. + \frac{e^{-Lpq_R} \cdot (q_R - m_-)^{1/2} \cdot S_+(q_R,p)}{|S(q_R,p)|} \right] \quad (60)$$

which holds for any $p < (\tau_m/h)$.

4.3. *Non-thermal limit case*

As a check of the present analysis, the non-thermal case $[\varepsilon = h = 0]$ worked out by Freund (1974, 1990) is now considered as a limit case. Freund, however, followed a different approach based on superposition. Then, the functional eqn (53) becomes

$$\Sigma^*_{y+}(q,p) - \frac{F \cdot e^{Lpq}}{p} = -\frac{\mu}{m^2} \frac{R(q)}{\alpha(q)} \cdot U^*_{y-}(q,p) \quad (61)$$

where $m \equiv (V_1/V_2) > 1$, $R(q) = 4q^2\alpha\beta + T^2$, $\alpha(q) \equiv \alpha = (1-q^2)^{1/2}$, $\beta(q) \equiv \beta = (m^2 - q^2)^{1/2}$, with $\pm q'_R \equiv \pm(V_1/V_R) > \pm m$ being the roots of the classical Rayleigh equation $R(q) = 0$. Further, eqn (54) gives

$$\Sigma^*_{y+}(q,p) = \frac{F \cdot (q + q'_R) \cdot S_+(q)}{2\pi i p (1+q)^{1/2}} \cdot \int_{-i\infty}^{i\infty} \frac{e^{Lp\omega}(1+\omega)^{1/2}}{(\omega + q'_R) \cdot S_+(\omega) \cdot (\omega - q)} d\omega \quad (q \text{ in } \mathrm{Re}(\omega) > 0)$$
$$(62)$$

where

$$S_\pm(\omega) = \exp\left(-\frac{1}{\pi} \cdot \int_1^m \tan^{-1} \left[\frac{4z^2(m^2 - z^2)^{1/2}(z^2 - 1)^{1/2}}{(m^2 - 2z^2)^2} \right] \cdot \frac{dz}{z \pm \omega} \right) \quad (63)$$

and the one-sided Laplace-transformed SIF is found as

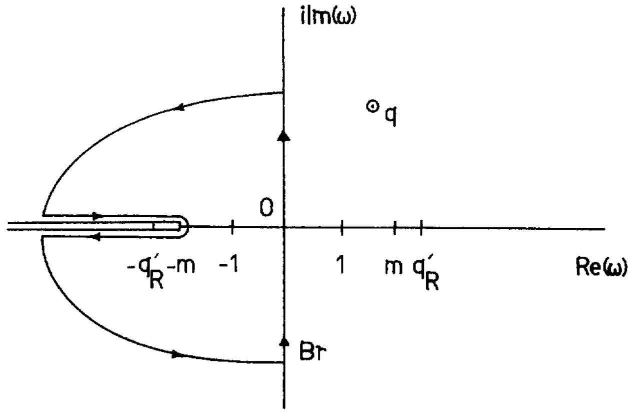

Fig. 11. Deformation of contour and branch cuts for the integral in eqn (62).

$$K_I(p)^{\text{classic}} = -\frac{2^{1/2}F}{\pi}\cdot\frac{1}{p^{1/2}}\cdot\int_m^\infty \frac{e^{-Lp\omega}(\omega-1)^{1/2}}{(\omega-q_R')\cdot S_-(\omega)}\,d\omega \tag{64}$$

by directly evaluating the Bromwich integral in eqn (62) through Cauchy's theory [see also Fig. 11 and notice the difference between the branch cuts, which are pertinent to the integrands in eqns (54) and (62)]. We also mention that an asymptotic procedure similar to eqn (59) was again utilized in arriving at eqn (64).

Finally, an exact one-sided LT inversion follows by invoking properties of convolution of transforms:

$$\frac{k_I(s \equiv V_1 t)^{\text{classic}}}{(2/\pi L)^{1/2}F} = -\frac{1}{\pi}\int_0^s \frac{H(w-mL)\cdot(w-L)^{1/2}}{(s-w)^{1/2}\cdot(w-q_R'L)\cdot S_-(w)}\,dw \tag{65}$$

where $k_I(s \equiv V_1 t)^{\text{classic}}$ denotes the stress intensity factor in the physical time domain for the non-thermal (purely elastic) limit case of problem (52), with $H()$ being the Heaviside step function and $S_-(w)$ given by

$$S_-(w) = \exp\left(-\frac{1}{\pi}\cdot\int_L^{mL}\tan^{-1}\left[\frac{4Z^2(m^2L^2-Z^2)^{1/2}(Z^2-L^2)^{1/2}}{(m^2L^2-2Z^2)^2}\right]\cdot\frac{dZ}{Z-w}\right). \tag{66}$$

Indeed, one may observe that eqn (65) is identical with eqn (24) in the paper by Freund (1974), so the latter result is recovered from the present, more general, analysis.

4.4. *Numerical results*

Again, the material constants of titanium are employed and $L = 0.05$ m is taken. Figure 12 shows the transformed normalized SIF $K_I(p)\cdot[(2/\pi L)^{1/2}F]^{-1} \equiv F_5$ vs $(Lp)^{-1}$ for real and positive values of p, where $K_I(p)$ is given by eqn (60). One could observe the different behavior for large $(Lp)^{-1}$ of the transformed normalized SIF in Fig. 12 (mechanical loading) as compared with the one in Figs 4 and 5 (thermal loading). As will be seen immediately, this is also reflected in the behavior of the stress intensity factor in the physical time domain for large time. Indeed, Fig. 13 presents the variation of the normalized SIF, $k_I(s \equiv V_1 t)\cdot[(2/\pi L)^{1/2}F]^{-1}$, with the normalized time $(V_1 t/L)$. This graph was obtained by a numerical inversion of eqn (60) via the Stehfest technique described previously. A strong spike of the SIF value at the time of the Rayleigh-wave arrival at the crack tip is again observed, but now the SIF tends to a finite steady-state limit. Finally, if one is interested in the SIF history for a *combined* thermal and mechanical loading, he/she should superimpose either graph 8 or 9 with graph 13. We chose to present these graphs separately because of

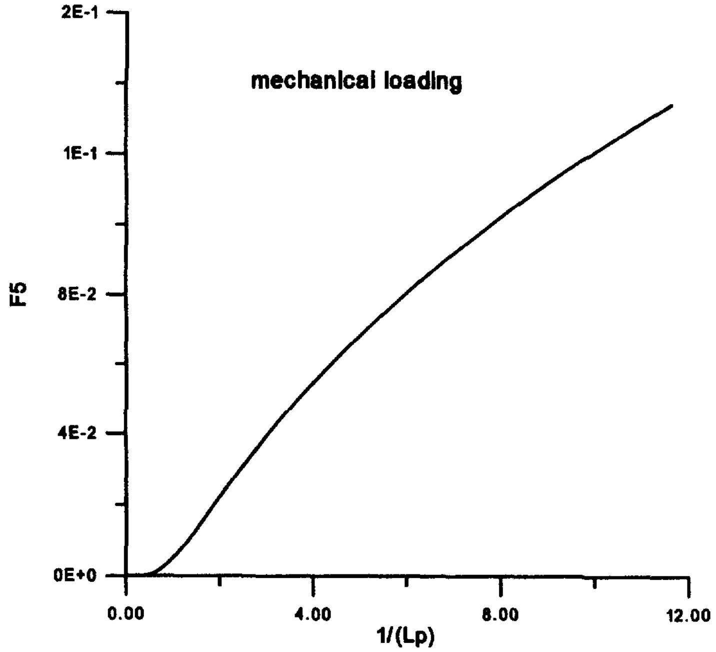

Fig. 12. Variation of the function $F_5 \equiv K_I(p) \cdot [(2/\pi L)^{1/2} F]^{-1}$ with $(Lp)^{-1}$.

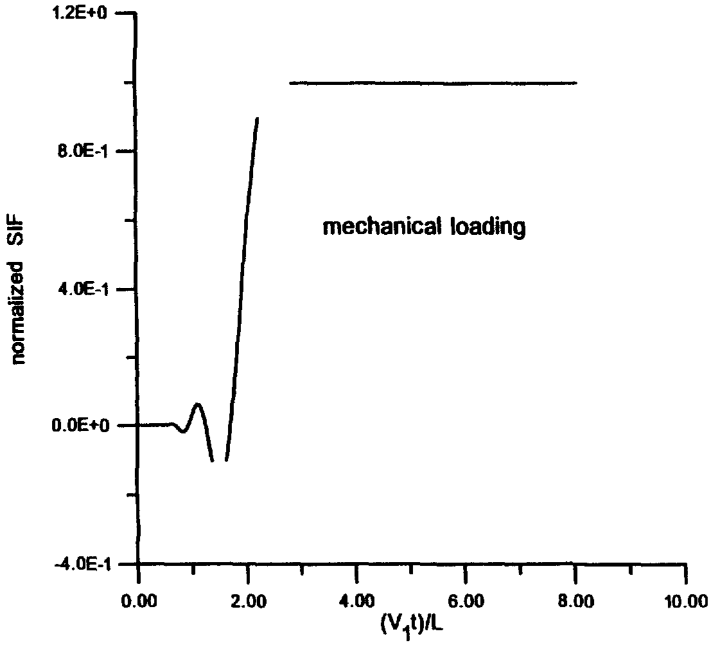

Fig. 13. History of the normalized SIF for mechanical loading.

(i) an obvious difficulty in defining a *unique* normalization (non-dimensionalization) for both cases, and (ii) different scales involved for the values of the stress intensity factors.

5. CONCLUDING REMARKS

The 2-D transient dynamic coupled-thermoelastic problem of the sudden thermal/mechanical loading of a cracked body was treated in the present work. In particular, a spatially non-uniform loading was considered along the crack faces in the form of concentrated thermal sources or sinks and/or concentrated forces. The solution procedure is based on one-sided (time) and two-sided (spatial) Laplace transforms, and on a newly developed analytic-function technique (Georgiadis and Brock, 1993) used to decouple two unknown functions in a single equation, which holds only along a vertical infinite line in the complex plane. The final one-sided LT inversion is done numerically through the well-established technique of Stehfest (1970).

Our results give the history of the stress intensity factor and show generally the interesting effect of the thermoelastic Rayleigh waves upon the severity of the crack-tip stress field. Also, the present solution provides the Green's function for thermoelastic cracked bodies subjected to more general spatially/temporally non-uniform loadings.

Acknowledgements—L.M. Brock and H.G. Georgiadis gratefully acknowledge the support of USA–NSF Grant DMS 9121700 to L.M. Brock. The work was partially carried out while H.G. Georgiadis was a visiting faculty member in the Department of Engineering Mechanics at the University of Kentucky.

REFERENCES

Achenbach, J. D. (1971) In *Mechanics Today*, ed. S. Nemat-Nasser, Vol. 1, pp. 1–57. Pergamon Press, Oxford.

Achenbach, J. D. (1973) *Wave Propagation in Elastic Solids*. North-Holland, NY.

Achenbach, J. D. and Brock, L. M. (1975) In *Dynamic Crack Propagation*, ed. G. C. Sih, pp. 529–541. Noordhoff, Leyden.

Ang, W. T. (1988) A crack in an anisotropic layered material under the action of impact loading. *ASME Journal of Applied Mechanics* **55**, 120–125.

Atkinson, C. (1977) In *Elastodynamic Crack Problems*, ed. G. C. Sih, pp. 213–248. Noordhoff, Leyden.

Atkinson, C. (1986) In *Applied Mechanics Update*, eds C. R. Steele and G. S. Springer, pp. 321–339. ASME, New York.

Atkinson, C. and Craster, R. V. (1992) Fracture in fully coupled dynamic thermoelasticity. *Journal of Mechanics and Physics of Solids* **40**, 1415–1432.

Barber, J. R. (1989) An asymptotic solution for short time transient heat conduction between two similar contacting bodies. *International Journal of Heat and Mass Transfer* **32**, 943–949.

Barber, J. R. and Comninou, M. (1983) The penny-shaped interface crack with heat flow: II. Imperfect contact. *ASME Journal of Applied Mechanics* **50**, 770–776.

Barber, J. R., Ben Ammar, F. and Georgiadis, H. G. (1989) Conductive heat exchange between bodies which are in contact for a very short period of time. In *Collected Papers in Heat Transfer*, eds W. J. Marner *et al.*, pp. 101–106. ASME, New York.

Biot, M. A. (1956) Thermoelasticity and irreversible thermodynamics. *Journal of Applied Physics* **27**, 240–253.

Boley, B. A. and Tolins, I. S. (1962) Transient coupled thermoelastic boundary value problems in the half-space. *ASME Journal of Applied Mechanics* **29**, 637–646.

Brock, L. M. (1975) The stresses and strain energy density near a crack edge due to P- and SV-wave diffraction. In *Developments in Mechanics*, eds C. W. Bert *et al.*, Vol. 8, pp. 125–139.

Brock, L. M. (1989a) An exact transient analysis of dislocation emission and fracture. *Journal of Mechanics and Physics of Solids* **37**, 47–69.

Brock, L. M. (1989b) Transient analyses of dislocation emission in the three modes of fracture. *International Journal of Engineering Science* **27**, 1479–1495.

Brock, L. M. and Wu, J.-S. (1990) Incident wave and dislocation acceleration effects in dislocation emission from cracks. *ASME Journal of Applied Mechanics* **57**, 870–876.

Brock, L. M. (1992) Transient thermal effects in edge dislocation generation near a crack edge. *International Journal of Solids and Structures* **29**, 2217–2234.

Brock, L. M. (1995a) Transient thermal response near dynamically-loaded cracks during dislocation generation. *Acta Mechanica* (accepted).

Brock, L. M. (1995b) Slip/diffusion zone formation at rapidly-loaded cracks in thermoelastic solids. *Journal of Elasticity* **40**, 183–206.

Carlson, D. E. (1972) Linear thermoelasticity. In *Handbuch der Physik*, ed. S. Flugge, Vol. VIa/2, pp. 297–345. Springer, Berlin.

Carrier, G. F., Krook, M. and Pearson, C. E. (1966) *Functions of a Complex Variable*. McGraw-Hill, New York.

Chadwick, P. (1960) Thermoelasticity: the dynamical theory. In *Progress in Solid Mechanics*, eds I. N. Sneddon and R. Hill, Vol. 1, pp. 263–328. North-Holland, Amsterdam.

Chen, E. P. and Sih, G. C. (1977) In *Elastodynamic Crack Problems*, ed. G. C. Sih, pp. 1–57. Noordhoff, Leyden.

Chen, T. C. and Weng, C. I. (1991) Coupled transient thermoelastic response in an edge-cracked plate. *Engineering Fracture Mechanics* **39**, 915–925.

Chen, C. K. and Kuo, B. L. (1994) Coupled transient thermoelastic contact problem in an edge-cracked plate. *ASME Journal of Applied Mechanics* **61**, 736–738.

Davies, B. and Martin, B. (1979) Numerical inversion of the Laplace transform: a survey and comparison of methods. *Journal of Composite Physics* **33**, 1–32.

Freund, L. B. (1974) The stress intensity factor due to normal impact loading of the faces of a crack. *International Journal of Engineering Science* **12**, 179–189.

Freund, L. B. (1990) *Dynamic Fracture Mechanics*. Cambridge University Press, Cambridge, MA.

Georgiadis, H. G., Barber, J. R. and Ben Ammar, F. (1991a) An asymptotic solution for short-time transient heat conduction between two dissimilar bodies in contact. *Quarterly Journal of Mechanics and Applied Mathematics* **44**, 303–322.

Georgiadis, H. G., Theocaris, P. S. and Mouskos, S. C. (1991b) Plane impact of a cracked viscoelastic body. *International Journal of Engineering Science* **29**, 171–177.

Georgiadis, H. G. (1993) Shear and torsional impact of cracked viscoelastic bodies—a numerical integral equation/transform approach. *International Journal of Solids and Structures* **30**, 1891–1906.

Georgiadis, H. G. and Brock, L. M. (1993) An exact method for cracked elastic strips under concentrated loads—time-harmonic response. *International Journal of Fracture* **63,** 201–214.

Georgiadis, H. G. and Brock, L. M. (1994) Exact elastodynamic analysis of some fracture specimen models involving strip geometries. *International Journal of Solids and Structures* **31,** 2599–2613.

Jiang, Q. and Knowles, J. K. (1989) On the direct determination of the near-tip stress field for the scattering of SH-waves by a crack. *International Journal of Fracture* **41,** 283–288.

Kassir, M. K., Phurkhao, P. A. and Bandyopadhyay, K. K. (1986) Some transient coupled thermoelastic crack problems. *Theoretical and Applied Fracture Mechanics* **6,** 197–206.

Knops, R. J. and Payne, L. E. (1970) On uniqueness and continuous dependence in dynamical problems of linear thermoelasticity. *International Journal of Solids and Structures* **6,** 1173–1184.

Kokini, K. and Long, M. A. (1988) Transient thermal fracture of cracked plates. *Experimental Mechanics* **28,** 373–381.

Lee, Y. J. and Freund, L. B. (1990) Fracture initiation due to asymmetric impact loading of an edge cracked plate. *ASME Journal of Applied Mechanics* **57,** 104–111.

Lessen, M. (1956) Thermoelasticity and thermal shock. *Journal of Mechanics and Physics of Solids* **5,** 57–61.

Massalas, C. V., Anagnostaki, E. and Kalpakidis, V. K. (1985) Some considerations on the coupled thermoelastic problems. *Letters of Applied Engineering Science* **23,** 677–683.

Nied, H. F. (1983) Thermal shock fracture in an edge-cracked plate. *Journal of Thermal Stresses* **6,** 217–229.

Nied, H. F. (1987) Thermal shock in an edge-cracked plate subjected to uniform surface heating. *Engineering Fracture Mechanics* **26,** 239–246.

Noble, B. (1958) *Methods Based on the Wiener–Hopf Technique*. Pergamon Press, New York.

Rajapakse, R. K. N. D. and Gross, D. (1995) Transient response of an orthotropic elastic medium with a cavity. *Wave Motion* **21,** 231–252.

Roos, B. W. (1969) *Analytic Functions and Distributions in Physics and Engineering*. Wiley, New York.

Stehfest, H. (1970) Numerical inversion of Laplace transforms. *Communications of ACM* **13,** 47–49, 624.

Viktorov, I. A. (1967) *Rayleigh and Lamb Waves*. Plenum Press, New York.